Effect of tension-compression asymmetry of AZ31B magnesium alloys on four-point bending

Émile Roux, Pascale Balland, Ludovic Charleux

Mechanics Research Communications xxx (xxxx) xxx

Contents lists available at ScienceDirect

Mechanics Research Communications

journal homepage: www.elsevier.com/locate/mechrescom

Effect of tension-compression asymmetry of AZ31B magnesium alloys on four-point bending

Emile Roux*, Pascale Balland, Ludovic Charleux

Univ. Savoie Mont Blanc, SYMME, FR-74000 Annecy, France

ARTICLE INFO

Article history:
Received 28 February 2020
Revised 17 October 2020
Accepted 5 February 2021
Available online xxx

Keywords:
Magnesium alloy
Four-point bending
AZ31B
Digital image correlation

ABSTRACT

The mechanical response of magnesium alloy AZ31B is addressed thanks to four-point bending tests. These alloys are known to have an asymmetrical behavior in tension-compression. The bending test is, therefore, a good candidate to analyze this effect because it combines the two solicitations. Digital image correlation is used to measure the evolution of the strain fields during the test. Measurements of the shift of the neutral line (zero strain) of the specimen are then presented for samples taken in the rolling direction and the transverse direction. It is shown that the shift of this line is initially towards the side in tension and then shifts back toward the center of the sample. Due to this reversal of the sliding direction of the neutral line, some physical points of the tested specimen are subjected alternatively to compression and tension. Measurements show that these alternations are confined to the elastic domain.

1. Introduction

The tension-compression asymmetry in the plastic flow of magnesium alloys is a well-known phenomenon. The microstructural origin of this phenomenon is well explained in the literature. This is due, on the one hand, to the limited number of active slip systems at room temperature in hexagonal close packed (HCP) metallic alloys such as magnesium and, on the other hand, to the twinning deformation mechanism which can contribute significantly to plastic deformation. These two phenomena depend on both the initial texture and loading path [1–4]. It leads to an asymmetry in strain hardening between tension and compression loading paths [5].

Bending tests are good candidates for demonstrating and analyzing the tension-compression asymmetry of such alloys because the test specimen is loaded in tension on one side and compression on the other. These tests are also a good way to study the formability of theses materials [6]. In [7], a clamped beam is tested at different temperatures and a digital image correlation (DIC) method is used to measure the evolution of the strain fields during loading to propose and validate a model. A V-bending test is also reported in [6] to analyze the fracture behavior of ZEK100 alloys. In [8], a four-point bending test with 6 strain gauges is performed on AZ31B samples and the asymmetry is confirmed by the observed residual stresses.

Under the hypothesis of the linear beam theory, the neutral strain line remains in the center of the sample, in large deformations, this is no longer the case. As reported by Huang et al. [9], for general metal material like aluminum with face-centered cubic structure, the neutral strain line moves to the compression region, which is not the case for magnesium alloys with HCP structure, the neutral line moves to the tension side. They used a V-bending test, the microstructure evolution is observed and linked with the shift of the neutral strain line of the bent beam.

The evolution of the neutral line is an observable data which seems relevant to qualify this asymmetry. In literature, the shift of the neutral strain line has never been observed accurately and continuously during the evolution of the bending. The approach developed in this work aims to provide new experimental data for modeling purposes and further constitutive modeling parameters identification of AZ31B alloys. The goal is to quantify the evolution of the position of the neutral strain line of the bent beam during the test by the means of the DIC method.

2. Experimental procedure

The tested material is an AZ31B magnesium alloy (Table 1) provided in a rolled sheet form with a thickness of 6mm. Two kinds of samples are tested: RD samples are machining with the long axis in the rolling direction, TD samples are machining with the long axis in the transverse direction. For the rest of the paper, the x-vector $\vec{x}$ represents the long axis of the specimen, whether it is taken from RD or TD.

* Corresponding author.

https://doi.org/10.1016/j.mechrescom.2021.103672
0093-6413/

Table 1
AZ31B chemical composition in %.

Al	Zn	Mn	Fe	Cu	Si	Ni	Mg
3.29	1.02	0.34	0.0022	0.0079	0.0082	0.0009	95.3308

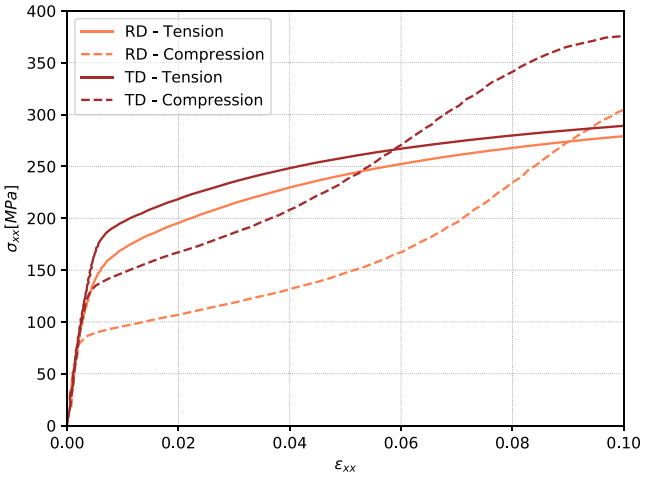

Fig. 1. Comparison of stress-strain curve for AZ31B alloy under uni-axial tension and uni-axial compression for Rolling Direction (RD) and Transverse Direction (TD) respectively.

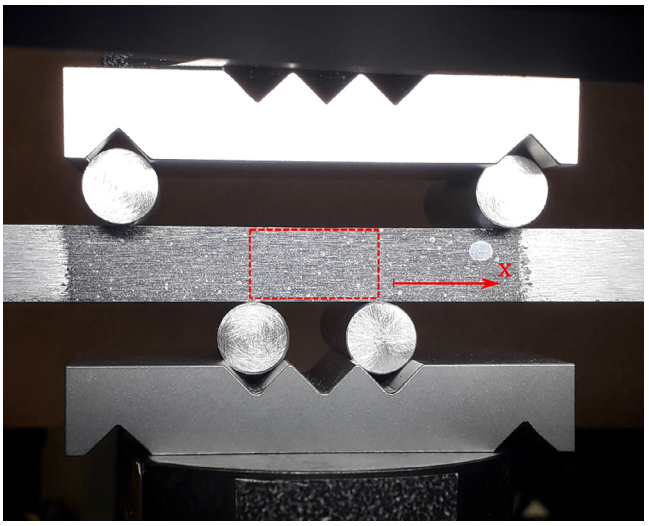

Fig. 2. 4-point bending setup with speckle pattern on the sample – the red dashed frame is the zone of interest (ZOI) for the DIC analysis. (For interpretation of the references to color in this figure legend, the reader is referred to the web version of this article.)

A comparison between compression and tension stress-strain responses for both directions (RD and TD) is presented in Fig. 1. The stress-strain curves are determined thanks to the large deformation theory with the Green-Lagrange strain formulation. The strains are measured locally using DIC method. The asymmetry in plastic flows between tension and compression is well visible. For the RD sample, the asymmetry is stronger than for the TD sample. At $\varepsilon = 2\%$, the ratio $\sigma_{comp}/\sigma_{tens} = 0.55$ in RD, and $\sigma_{comp}/\sigma_{tens} = 0.77$ in TD. The flow stress is lower in compression (dashed lines in Fig. 1) for strain lower than 8.8% for RD samples and lower than 5.8% for TD samples, and greater after hand. Those observations agree with [4,8].

A four-point bending setup [10] is used to load the sample (see Fig. 2). The distance between the inner pins is equal to 20mm and between the outer pins is equal to 60mm. The upper pins moved downward of 5 mm at a constant velocity of 1mm.s^{-1}, the lower pins are fixed. The tested samples have a thickness of 6mm, a height of 12.5mm and a length of 200mm. The tests are carried out on an INSTRON 5569 tensile machine fitted with a load cell of 50 kN. A black and white speckle is sprayed on the side of the sample, the pattern can be seen in Fig. 2.

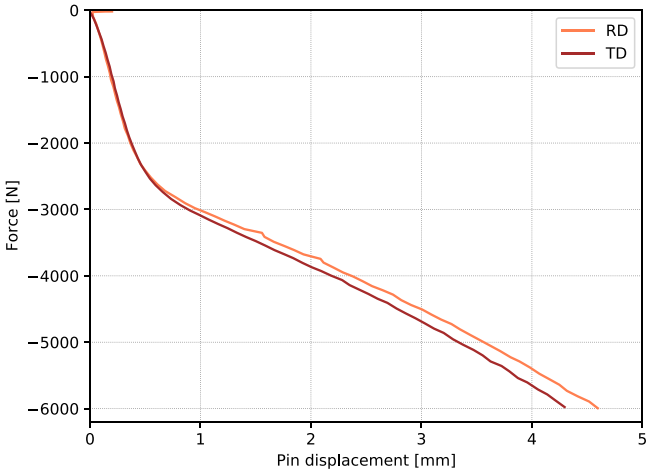

Fig. 3. Bending force evolution for DR and TD samples.

Images are taken using a SVS camera (EXO252MU3) with a focal of 12mm, the resolution is 2048 by 1536 pixels.

Imaging and force measurements are synchronized. The image capture is driven by the change in force: one image is captured every 100N. DIC method is then used to determine the displacement fields, the strain fields at the surface of the sample [11] and the displacement of the moving pins. For DIC methods the uncertainty in displacement measurement is equal to 0.01 pixel. In taken images, the height of the sample represents 360 pixels. The distance between pixels is 35µm, therefore the error in displacement measurement is less than 0.5µm. To perform the DIC analyze subsets of 20 pixels by 20 pixels are used, without overlapping. The computed strains are not filtered.

The force recorded during the bending tests is plotted in Fig. 3. TD sample logically requires a higher force than the RD sample to be bent. This is in agreement with the results of the uni-axial test curves (Fig. 1). But the difference is not as significant as the difference observed in uni-axial test. This low sensitivity toward anisotropy effects may be explained by the fact that the mechanical state is more complex in bending. The elastic and plastic regimes in tension and compression are present together. The two regimes (elastic and plastic) are visible on both curves (Fig. 3).

The transition between the two regimes takes place at a value of about 0.8mm of pins displacement. Fig. 4 show the obtained strain fields by DIC in the zone of interest (ZOI) for the RD sample. The strain field is displayed at different stages of bending. The strain iso-value lines are shown in each figure. The neutral line is the zero-strain line, it can be seen at different stages of bending.

3. Results and discussion

Fig. 4 shows the strain field ε_{xx} for the RD sample at different stages of bending (upper pins displacement = 0.8mm, 2mm, and 4mm). Fig. 4a shows the strain field at the beginning of the plastic regime. The shift of the neutral line to the tension side is visible. Graphs b and c of the same figure (Fig. 4) also show this shift for more advanced bending stages. For a 4mm pins displacement (Fig. 4c) the tension strain reaches a maximum value of 4% while

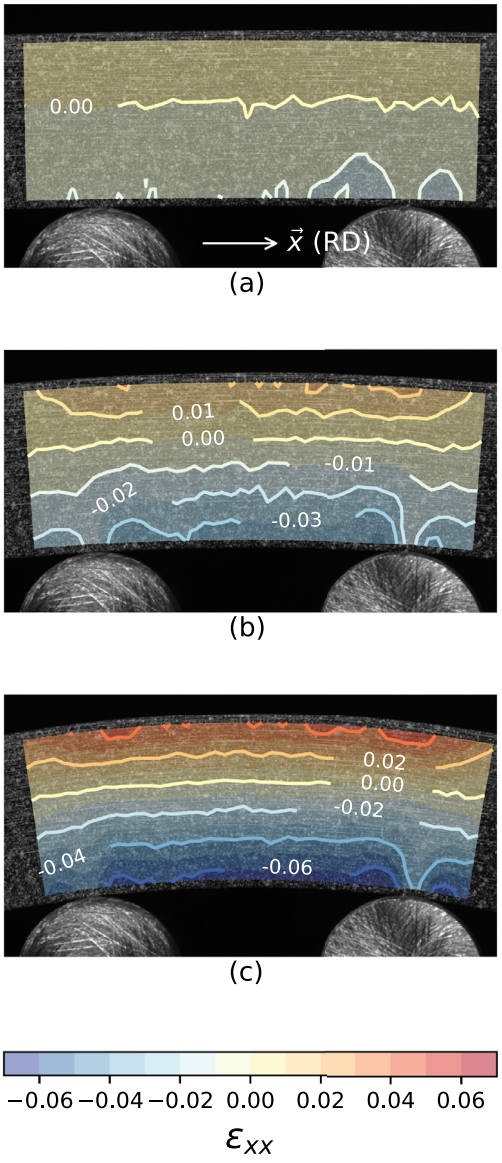

Fig. 4. Strain field ε_{xx} measured by DIC on the RD sample – (a) pins displacement = 0.8mm, (b) pins displacement = 2mm, (c) pins displacement = 4mm.

compression strain reaches −6%. For the TD sample, the strain field is almost similar. That is why it is not shown.

The position of the neutral line evolves during the bending test. For each image, a linear regression based on the strain ε_{xx} measured in the central third of the ZOI is calculated. The regression is calculated with respect to the initial undeformed configuration. Therefore the coordinates system used to construct Fig. 5 refer to the coordinate system linked to the undeformed configuration.

The central third of the ZOI is an area where the strain field is not perturbed by the contact with the pins. The perturbation due to contact with the pins can be seen in Fig. 4c for example. This regression is then used to calculate the position of the neutral line on each image. The use of linear regression allows limiting measurement noise.

This procedure is applied for each taken picture, the evolution of the position of the neutral line (which is the isostrain lines equal to 0) for RD and TD samples are plotted in Fig. 5 vs. upper pins displacement. Additionally, the evolution of the position of the isostrain lines equal to 0.4% and −0.2% are extracted thanks to the same method for the RD sample. ($\varepsilon_{xx} = 0.4\%$ and $\varepsilon_{xx} = -0.2\%$ are respectively the elastic strain limit under uni-axial tension and uni-axial compression (see Fig. 1)).

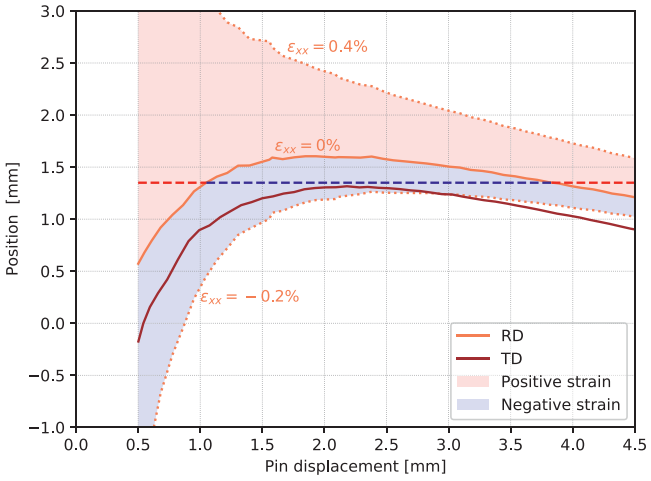

Fig. 5. Neutral line shifting during bending for RD and TD samples (solid lines). For the RD specimen, the position of the isolines $\varepsilon_{xx} = 0.4\%$ and $\varepsilon_{xx} = -0.2\%$ are plotted. These dashed lines correspond respectively to the elastic strain limit under uni-axial tension and uni-axial compression of the material in the RD direction. These two lines allow representing the elastic strain domain (red area for positive strain and blue area for negative strain). Additionally the loading path of one physical point is highlighted (large dashed line). (For interpretation of the references to color in this figure legend, the reader is referred to the web version of this article.)

The shift of neutral lines follows the same trend for both samples (Fig. 5). As the bending progresses, the neutral line first shifts rapidly to the tension side, then reaches a maximum and then returns towards the center of the specimen. This shift is linked to the tension-compression asymmetry of the plastic flow. The yield stress in compression is lower than in tension, it makes the deformation easier in the compression side of the sample. It results in a shift of the neutral line strain toward the tension side of the sample. In a later stage of the deformation, the difference between compression and tension is less pronounced (Fig. 1), this reduction of the asymmetry results in a backward shift of the neutral line toward the center of the sample.

The TD specimen shows a smaller deviation of the neutral line than the RD one. This difference can be explained by the difference of tension-compression asymmetry of the material in the two directions (RD or TD, Fig. 1). The tension-compression asymmetry is more pronounced for the RD sample, resulting in a stronger shift of the neutral line.

The shift and the shift-backward of the neutral line are seen in both directions (RD and TD). It means that a central part of the sample is loaded alternatively in tension and compression. For example, the physical point at +1.3mm of the center of the sample (large dashed line in Fig. 5, is loaded under tension for pins displacement up to 1mm (first red part of the line), then is loaded under compression up to a pins displacement of 3.8mm (blue part of the line), and is loaded back in tension after hand (second red part of the line). Therefore by following horizontal lines from left to right in Fig. 5, the loading path of each physical point can be analyzed. In Fig. 5, the evolution of isostrain line of 0.4% and −0.2% are added. These values correspond respectively to the elastic strain limit under uni-axial tension and uni-axial compression in the RD direction (see Fig. 1). The addition of the elastic domain envelope shows that there are no material points (i.e. no horizontal lines) that undergo alternately plastic strain in tension and plastic strain in compression.

Only alternating strain in the elasticity domain is observed. The alternation in the plastic domain is not observed in these tests,

but by extrapolation, it can be supposed that it could appear if the bending is more pronounced.

4. Conclusion

Four-point bending tests were conducted on AZ31B specimens. These specimens were machined in the rolling direction (RD) and the transverse direction (TD) to see the impact of anisotropy. As this alloy is weakly anisotropic the bending results are quite close in both directions. The bending test was instrumented with DIC method to have a fine representation of the strain fields during the test. These measurements made it possible to highlight :

- an asymmetrical development of the strain between the tension and compression sides.
- a shift of the neutral line towards the tension side at the beginning of bending and then a backward shift of this neutral line towards the center of the specimen.
- that some physical areas of the sample alternately undergo strains in tension and later in compression (these strains remain in the elastic range for the carried out tests).

These very fine experimental tests could be used to validate any behavior modeling qualitatively.

The experimental results presented here could be used to qualitatively validate material behavior predicted by computational models.

Declaration of Competing Interest

The authors declare that they have no conflict of Interest regarding the work presenter in the article entitled: Effect of tension-compression asymmetry of AZ31B magnesium alloys on four-point bending, by Emile Roux, Pascale Balland and Ludovic Charleux.

References

[1] N. Chandola, R.A. Lebensohn, O. Cazacu, B. Revil-Baudard, R.K. Mishra, F. Barlat, Combined effects of anisotropy and tension–compression asymmetry on the torsional response of AZ31 mg, Int. J. Solids Struct. 58 (2015) 190–200, doi:10.1016/j.ijsolstr.2015.01.001.
[2] D. Ghaffari Tari, M.J. Worswick, U. Ali, M.A. Gharghouri, Mechanical response of AZ31B magnesium alloy: experimental characterization and material modeling considering proportional loading at room temperature, Int. J. Plast. 55 (2013) 247–267, doi:10.1016/j.ijplas.2013.10.006.
[3] S.A. Habib, A.S. Khan, T. Gn, Aupel-Herold, J.T. Lloyd, S.E. Schoenfeld, S.A. Habib, Anisotropy, tension-compression asymmetry and texture evolution of a rare-earth-containing magnesium alloy sheet, ZEK100, at different strain rates and temperatures: experiments and modeling, Int. J. Plast. 95 (2017) 163–190, doi:10.1016/j.ijplas.2017.04.006.
[4] W. Muhammad, M. Mohammadi, J. Kang, R.K. Mishra, K. Inal, An elasto-plastic constitutive model for evolving asymmetric/ anisotropic hardening behavior of AZ31B and ZEK100 magnesium alloy sheets considering monotonic and reverse loading paths, Int. J. Plast. 70 (2015) 30–59, doi:10.1016/j.ijplas.2015.03.004.
[5] N.V. Dudamell, I. Ulacia, F. Gálvez, S. Yi, J. Bohlen, D. Letzig, I. Hurtado, M.T. Pérez-Prado, Influence of texture on the recrystallization mechanisms in an AZ31 Mg sheet alloy at dynamic rates, Mater. Sci. Eng., A 532 (2012) 528–535, doi:10.1016/j.msea.2011.11.018.
[6] I. Aslam, B. Li, Z. Mcclelland, S.J. Horstemeyer, Q. Ma, P.T. Wang, M.F. Horstemeyer, Three-point bending behavior of a ZEK100 Mg alloy at room temperature, Mater. Sci. Eng. A 590 (2013) 168–173, doi:10.1016/j.msea.2013.10.030.
[7] S. Härtel, M. Graf, T. Lehmann, M. Ullmann, Influence of tension-compression anomaly during bending of magnesium alloy AZ31, Mater. Sci. Eng. 705 (2017) 62–71, doi:10.1016/j.msea.2017.08.066.
[8] J.P. Nobre, U. Noster, M. Kornmeier, A.M. Dias, B. Scholtes, Deformation asymmetry of AZ31 wrought magnesium alloy, in: Key Engineering Materials, 230–232, 2002, pp. 267–270. www.scientific.net/kem.230-232.267
[9] G. Huang, L. Wang, H. Zhang, Y. Wang, Z. Shi, F. Pan, Evolution of neutral layer and microstructure of AZ31b magnesium alloy sheet during bending, Mater. Lett. 98 (2013) 47–50, doi:10.1016/j.matlet.2013.02.055.
[10] M.E. Nixon, R.A. Lebensohn, O. Cazacu, C. Liu, Experimental and finite-element analysis of the anisotropic response of high-purity a-titanium in bending, Acta Mater. 58 (17) (2010) 5759–5767, doi:10.1016/j.actamat.2010.06.051.
[11] P. Vacher, S. Dumoulin, F. Morestin, S. Mguil-Touchal, Bidimensional strain measurement using digital images, Proc. Inst. Mech.Eng. Part C 213 (8) (1999) 811–817, doi:10.1243/0954406991522428.